A VOLUME INTEGRAL CODE FOR EDDY-CURRENT NONDESTRUCTIVE EVALUATION

Harold A. Sabbagh
John R. Bowler
L. David Sabbagh

Sabbagh Associates, Inc.
4639 Morningside Drive
Bloomington, IN 47401

ABSTRACT

This paper is an extension of J. R. Bowler, H. A. Sabbagh, and L. D. Sabbagh, "A Computational Model of Eddy-Current Probes Over a Stratified Composite Workpiece", which was presented at the 4th Annual Review of Progress in Applied Computational Electromagnetics, Monterey, CA, March 1988. It describes an application of modern methods of computational electromagnetics to the problem of eddy-current nondestructive evaluation (NDE). Specifically, a volume integral equation is developed that can be used to model eddy-current probes with ferrite cores, or it can be used to compute flaw-field interactions. Both of these problems are of considerable importance in applying electromagnetic techniques to NDE, for they are intimately involved in detecting flaws, and inverting eddy-current data for reconstructing flaws.

The model is fully three-dimensional, and the discretized integral equation is solved iteratively using conjugate gradients and FFT techniques. Problems with 12,000 unknowns are being routinely solved on the Alliant FX/1 minisupercomputer in reasonable times. The model is used to compute such important probe parameters as impedance and coupling. It is also used to compute the electromagnetic response of flaws as the geometry of the flaw changes, or as a function of frequency.

I. INTRODUCTION

The design of eddy-current probe coils is important in the quantitative nondestructive evaluation (NDE) of such widely disparate materials as advanced composites (such as graphite-epoxy) to zirconium. Much of the present state of the art in the design of such probes is empirical, or based on elementary circuit-theoretic models. These models do not yield as much information as a designer needs, even when the workpiece is a 'classical material', such as stainless steel. In the presence of the newer composite materials, the problem becomes exacerbated because a large proportion of these are anisotropic, and many of the conventional design rules-of-thumb become useless.

Another challenging problem facing the eddy-current NDE community is that of accurately predicting flaw-field interactions. Solving this problem is a necessary first step in developing inversion algorithms that will allow one to infer the nature of the flaw, given the probe response.

We are developing a computational model and code that will effectively solve both problems. It will, for example, allow the designer of probes to compute fields within a multi-layer composite workpiece, and to determine such important probe parameters as impedance and coupling. The model is fully three-dimensional and will include the effects of ferrite cores and shielding. In addition, it is currently being used to compute a variety of flaw responses, such as impedance changes, as a function of flaw parameters and frequency.

The model is based on a volume integral equation that is solved iteratively using conjugate gradients and FFT techniques. Problems with 12,000 unknowns are being routinely solved on the Alliant FX/1 minisupercomputer in reasonable times. We believe that the flexibility and simplicity required of such a model and code effectively rules out other candidate techniques, such as finite elements and boundary integral equations.

In this paper we will briefly outline the electromagnetic and computational aspects of the model and code, as it is applied to ferrite core probes and flaw-field interactions. In addition, we will describe the first validation steps, which involve comparison with other codes, as well as comparison with experimental data.

II. FERRITE-CORE PROBE MODEL

(a) Integral Equation for the Magnetization

In previous work [1-4], we have developed a model of a ferrite-core probe over a planar stratified workpiece as illustrated in Figure 1. In this model, which was developed for NDE, the field computations require the known currents in the coils and the unknown 'Amperian currents' due to the magnetization of the ferrite core. Hence, we include a magnetic current source, $\mathbf{J}_m = -j\omega\mu_0\mathbf{M}$ to account for the presence of the ferrite. With two distinct current source types, and the surface of the workpiece in the plane $z = 0$, the magnetic field has the form

$$\mathbf{H}(\mathbf{r}) = \int_{coil+core} [\mathbf{G}^{(me)}(\mathbf{r}|\mathbf{r}') \cdot \mathbf{J}_e(\mathbf{r}') + \mathbf{G}^{(mm)}(\mathbf{r}|\mathbf{r}') \cdot \mathbf{J}_m(\mathbf{r}')]d\mathbf{r}', \tag{1}$$

$\mathbf{J}_e$ being the coil current. The first superscript on the Green's tensors, $\mathbf{G}^{(me)}$ and $\mathbf{G}^{(mm)}$, indicates the type of field (m for magnetic and e for electric) and the second the nature of the source current. These tensors depend partly on the structure and material properties of the workpiece, since such factors will determine the reflected field. In fact all the relevant effects of the workpiece are embodied in a set of reflection coefficients contained in the above Green's functions. In the

most general case that we have encoded, a laminated composite material is modeled as a multi-layered anisotropic slab structure, and the reflection coefficients computed accordingly. Simpler structures can also be accommodated; for example, by putting the reflection coefficients to zero, we compute the magnetisation of the core in free space.

The first term under the integral in (1) is the incident magnetic field, $\mathbf{H}^{(i)}$, produced by the prescribed electric currents in the coil. $\mathbf{H}^{(i)}$ is given independently of the ferrite core and is therefore independent of $\mathbf{M}$ or $\mathbf{J}_m$. Hence, assuming a nonconducting core,

$$\mathbf{H}(\mathbf{r}) = \mathbf{H}^{(i)}(\mathbf{r}) + \int_{core} \mathbf{G}^{(mm)}(\mathbf{r}|\mathbf{r}') \cdot \mathbf{J}_m(\mathbf{r}')d\mathbf{r}'. \tag{2}$$

Our aim is to define a volume integral equation for computing the core magnetization, preferably in such a way that a numerical solution can be found even in cases where the ferrite permeability is infinite. In most practical situations the relative permeabilty of the ferrite used in eddy-current probes is fairly large, typically in the range 200 to 2000, and it is useful to get infinite permeability solutions for comparison. To derive the desired equation, we put $\mathbf{H}(\mathbf{r}) = \mathbf{B}(\mathbf{r})/\mu_0 - \mathbf{M}(\mathbf{r})$, so that (2) becomes

$$\begin{aligned} \frac{\mathbf{B}^{(i)}(\mathbf{r})}{\mu_0} &= \frac{\mathbf{B}(\mathbf{r})}{\mu_0} - \mathbf{M}(\mathbf{r}) + j\omega\mu_0 \int_{core} \mathbf{G}^{(mm)}(\mathbf{r}|\mathbf{r}') \cdot \mathbf{M}(\mathbf{r}')d\mathbf{r}' \\ &= \frac{\mathbf{B}(\mathbf{r})}{\mu_0} + j\omega\mu_0 \int_{core} \left[\mathbf{G}^{(mm)}(\mathbf{r}|\mathbf{r}') - \frac{\delta(\mathbf{r}-\mathbf{r}')}{j\omega\mu_0}\mathbf{I}\right] \cdot \mathbf{M}(\mathbf{r}')d\mathbf{r}', \end{aligned} \tag{3}$$

$\mathbf{I}$ being the unit tensor. Then multiplying (3) by $\nu = (1 - \mu_0/\mu)$, and using the fact that $\mathbf{M} = (\mathbf{B}/\mu_0)(1 - \mu_0/\mu)$, gives

$$\mathbf{M}^{(i)}(\mathbf{r}) = \mathbf{M}(\mathbf{r}) + j\omega\mu_0\nu(\mathbf{r}) \int_{core} \left[\mathbf{G}^{(mm)}(\mathbf{r}|\mathbf{r}') - \frac{\delta(\mathbf{r}-\mathbf{r}')}{j\omega\mu_0}\mathbf{I}\right] \cdot \mathbf{M}(\mathbf{r}')d\mathbf{r}'. \tag{4}$$

This is the basic integral equation for the magnetization vector. Its solution is the starting point for determining the fields and driving-point impedance of the ferrite core.

The Green's function can be written in the form of a two-dimensional Fourier transform

$$\mathbf{G}^{(mm)}(x-x', y-y', z, z') = \iint_{-\infty}^{\infty} \widetilde{\mathbf{G}}^{(mm)}(k_x, k_y; z, z')e^{-j[k_x(x-x')+k_y(y-y')]}dk_x dk_y. \tag{5}$$

When this is substituted into (4) the integrals over x' and y' become Fourier transforms, and the resulting integral equation for the magnetization becomes:

$$\begin{aligned} &\mathbf{M}^{(i)}(\mathbf{r}) = \mathbf{M}(\mathbf{r}) + \\ &\quad j\omega\mu_0\nu(\mathbf{r}) \int dz' \iint_{-\infty}^{\infty} \left[\widetilde{\mathbf{G}}^{(mm)}(k_x, k_y; z, z') - \frac{\delta(z-z')}{j\omega\mu_0}\mathbf{I}\right] \cdot \widetilde{\mathbf{M}}(k_x, k_y; z')e^{-j(k_x x + k_y y)}dk_x dk_y \end{aligned} \tag{6}$$

Note that ν vanishes for a core region with the free space permeability, and is equal to 1.0 when the permeability is infinite.

The Green's function consists of two parts: a free-space part, which ignores the presence of the slab, and a part which transforms the source into the reflected field. The free-space part, in turn, consists of two parts, $\widetilde{\mathbf{G}}_{(0)}^{(mm)}$, and a 'depolarization' term, $\widetilde{\mathbf{G}}_{(d)}^{(mm)}$. $\widetilde{\mathbf{G}}_{(0)}^{(mm)}$ is given by

$$\tilde{\mathbf{G}}_{(0)}^{(mm)}(k_x,k_y;z,z') = j\omega\epsilon_0 \begin{bmatrix} 1-k_x^2/k_0^2 & -k_xk_y/k_0^2 & \pm jk_x\lambda_0/k_0^2 \\ -k_xk_y/k_0^2 & 1-k_y^2/k_0^2 & \pm jk_y\lambda_0/k_0^2 \\ \pm jk_x\lambda_0/k_0^2 & \pm jk_y\lambda_0/k_0^2 & 1+\lambda_0^2/k_0^2 \end{bmatrix} \frac{e^{-\lambda_0|z-z'|}}{2\lambda_0}, \tag{7}$$

where the (+) sign goes with $z > z'$, (−) with $z < z'$, and $\lambda_0 = (k_x^2 + k_y^2 - k_0^2)^{1/2}$. The depolarization term is given by

$$\tilde{\mathbf{G}}_{(d)}^{(mm)}(k_x,k_y;z,z') = -j\frac{\delta(z-z')}{\omega\mu_0}\mathbf{a}_z\mathbf{a}_z. \tag{8}$$

The reflected Green's function is defined in terms of reflection coefficients, R_{xx}, R_{xy}, etc., whose values depend upon the nature of the slab and are independent of the location of the source and field points. Thus, the reflected Green's function has the general structure

$$\tilde{\mathbf{G}}_{(r)}^{(mm)}(k_x,k_y;z,z') = \begin{bmatrix} R_{xx} & R_{xy} & R_{xz} \\ R_{yx} & R_{yy} & R_{yz} \\ R_{zx} & R_{zy} & R_{zz} \end{bmatrix} e^{-\lambda_0(z+z')}. \tag{9}$$

The $x-x'$ and $y-y'$ dependence of the complete Green's tensor, $\mathbf{G}^{(mm)}$, implies that the source integration, (4), is a convolution in x and y. In addition, the free space Green's tensor has a $z-z'$ dependence, while the reflection Green's term has a $z+z'$ dependence. Therefore (4) contains the sum of a convolution and a correlation in z. In designing a numerical algorithm for computing M from a discrete version of (4), we have taken full advantage of this convolutional/correlational structure.

(b) Discretization of the Integral Equation by Taking Moments

The discretization of the integral equation (4) is done by subdividing the region of space occupied by the core into N_z layers, each of depth δ_z, and then expanding the magnetization vector and the permeabilty function, ν, using pulse functions. Thus,

$$\mathbf{M}(x,y,z) = \sum_{l=0}^{N_x}\sum_{m=0}^{N_y}\sum_{j=0}^{N_z} \mathbf{I}_{lmj} P_l(\frac{x}{\delta_x}) P_m(\frac{y}{\delta_y}) P_j(\frac{z-z_0}{\delta_z}), \tag{10}$$

and

$$\nu(x,y,z) = \sum_{l=0}^{N_x}\sum_{m=0}^{N_y}\sum_{j=0}^{N_z} \nu_{lmj} P_l(\frac{x}{\delta_x}) P_m(\frac{y}{\delta_y}) P_j(\frac{z-z_0}{\delta_z}), \tag{11}$$

where z_0 is the perpendicular distance from the workpiece to the bottom of the source grid, and the pulse functions satisfy

$$P_k(s) = \begin{cases} 1, & \text{if } k \le s < k+1.0; \\ 0, & \text{otherwise.} \end{cases} \tag{12}$$

We are going to use Galerkin's variant of the method of moments to complete the discretization. In Galerkin's method, we 'test' integral equation (4) with the same pulse functions that we used to expand the unknown, M, in (10). That is, we form moments of (4) by multiplying (6) by $P_l(\frac{x}{\delta_x})P_m(\frac{y}{\delta_y})P_j(\frac{z-z_0}{\delta_z})$, with M given by (10), and then integrating with respect to x, y, and z over each cell. This yields a linear system for $\mathbf{I}_{lmj}$:

$$\mathbf{I}^{(i)}_{lmj} = \delta_z \mathbf{I}_{lmj} + \nu_{lmj} \sum_{J=0}^{N_z} \sum_{L=0}^{N_x} \sum_{M=0}^{N_y} \mathbf{G}_{jJ}(l-L, m-M) \cdot \mathbf{I}_{LMJ}, \tag{13}$$

where

$$\mathbf{G}_{jJ}(l-L, m-M) = j\omega\mu_0 \delta_x \delta_y / 4\pi^2 \iint_{-\infty}^{\infty} e^{-j[k_x\delta_x(l-L)+k_y\delta_y(m-M)]} \tilde{\tilde{\Gamma}}^{(mm)}_{jJ}(k_x, k_y) \left[\frac{\sin(k_x\delta_x/2)}{k_x\delta_x/2}\right]^2 \left[\frac{\sin(k_y\delta_y/2)}{k_y\delta_y/2}\right]^2 dk_x dk_y \tag{14}$$

$\tilde{\tilde{\Gamma}}^{(mm)}_{jJ}$ is defined as

$$\tilde{\tilde{\Gamma}}^{(mm)}_{kj}(k_x, k_y) = \int_{z_{k-1}}^{z_k} dz \int_{z_{j-1}}^{z_j} dz' \left[\tilde{\mathbf{G}}^{(mm)}(k_x, k_y; z, z') - \frac{\delta(z-z')}{j\omega\mu_0}\mathbf{I}\right], \tag{15}$$

upon letting $z_j = z_0 + j\delta_z$; $j = 1, \ldots, N_z$.

As well as being of Toeplitz form in (l, L) and (m, M), the matrix of coefficients, (14), decomposes into two matrices, one of which has the Toeplitz form in (j, J) and the other has a Hankel form in (j, J). This structure, which is a direct consequence of the convolutional/correlational nature of the basic integral equation, allows us to use the fast Fourier transform for computing the result of multiplying an arbitrary vector by the matrix. It is important that this operation be carried out efficiently since it is used repeatedly in the conjugate gradient procedure.

III. FIELD-FLAW MODEL

The theory for the field-flaw interaction model is the dual of the preceding one for the magnetization. Instead of thinking of the core as being a magnetic perturbation of free-space, as in (2), we think of the flaw as being an electrical perturbation of the material half-space, as in Figure 2. Then (2) is replaced by

$$\mathbf{E}(\mathbf{r}) = \mathbf{E}^{(i)}(\mathbf{r}) + \int_{flaw} \mathbf{G}^{(ee)}(\mathbf{r}|\mathbf{r}') \cdot \mathbf{J}_a(\mathbf{r}') d\mathbf{r}', \tag{16}$$

where $\mathbf{J}_a$ is now the anomalous electric current due to the flaw, and $\mathbf{E}^{(i)}$ is the incident electric field at the flaw, due to the exciting coil, which is in free-space above the half-space. The electric-electric Green's function, $\mathbf{G}^{(ee)}$, is the electric field response, within the material half-space, to a point source of electric current, also within the half-space.

With these differences noted, the discretization of the integral equation proceeds as before, with the result that we arrive at another version of (13):

$$\mathbf{I}^{(i)}_{lmj} = \delta_z \mathbf{I}_{lmj} + \sigma_{lmj} \sum_{J=0}^{N_z} \sum_{L=0}^{N_x} \sum_{M=0}^{N_y} \mathbf{G}_{jJ}(l-L, m-M) \cdot \mathbf{I}_{LMJ}. \tag{17}$$

Here $\mathbf{I}^{(i)}_{lmj}$ is the incident anomalous electric current density, and σ_{lmj} is the anomalous electrical conductivity of the flaw. Also, the $\mathbf{G}$ matrix of (17) is derived using (14), except that the electric-electric Green's function is used, instead of the magnetic-magnetic.

By adopting the exciting current as the phase reference, the probe impedance, ΔZ, due to the flaw can be expressed in terms of the electric field, $\mathbf{E}^{(s)}$, scattered by the flaw as

$$I^2 \Delta Z = -\int_{coil} \mathbf{E}^{(s)}(\mathbf{r}) \cdot \mathbf{J}_e(\mathbf{r}) d\mathbf{r}. \tag{18}$$

One could use (18) directly to compute the probe response, but this would entail the intermediate step of calculating the scattered field at the coil before integrating over the coil region to get the impedance. Instead, we apply a reciprocity theorem relating the scattered field at the primary source (the eddy-current probe) to the incident field at the secondary source (the anomalous flaw current). Thus,

$$I^2 \Delta Z = -\int_{flaw} \mathbf{E}^{(i)}(\mathbf{r}) \cdot \mathbf{J}_a(\mathbf{r}) d\mathbf{r}. \tag{19}$$

This is the form used in the code.

A theory of eddy-current interaction with very thin (i.e., 'closed') cracks can also be developed using a form of surface integral equation [5]. This is one problem where a surface integral approach may be potentially superior to a volume integral model. The surface integral equation can be discretized via the method of moments, just as is the volume integral equation.

IV. THE CONJUGATE GRADIENT ALGORITHM

When we interpret (13) as a vector-matrix equation, then, clearly, ν_{lmj} are row-multipliers. Let us write this vector-matrix equation as the operator equation

$$Y = \mathcal{A}X, \tag{20}$$

where

$$Y = \mathbf{I}^{(i)}_{lmj}, \tag{21}$$

and

$$\mathcal{A}I = \delta_z \mathbf{I}_{lmj} + \nu_{lmj} \sum_{J=0}^{N_x} \sum_{L=0}^{N_z} \sum_{M=0}^{N_y} \mathbf{G}_{jJ}(l-L, m-M) \cdot \mathbf{I}_{LMJ}. \tag{22}$$

We will need the adjoint operator, $\mathcal{A}^*$, which corresponds to the conjugate transpose of the matrix:

$$\mathcal{A}^* I = \delta_z \mathbf{I}_{lmj} + \sum_{J=0}^{N_x} \sum_{L=0}^{N_z} \sum_{M=0}^{N_y} \mathbf{G}^{\dagger}_{J_j}(L-l, M-m) \cdot \nu_{LMJ} \mathbf{I}_{LMJ}. \tag{23}$$

The symbol † denotes the conjugate-transpose of a dyadic. Note that ν_{lmj} are real numbers.

The conjugate gradient algorithm [6,7] starts with an initial guess, X_0, from which we compute $R_0 = Y - \mathcal{A}X_0$, $P_1 = Q_0 = \mathcal{A}^* R_0$. In addition, we have a convergence parameter, ϵ. Then for $k = 1, 2, \ldots$, if $Test = \|R_k\|/\|Y\| < \epsilon$, stop; X_k is the optimal solution of (20). Otherwise, update X_k by the following steps:

$$\begin{aligned} S_k &= \mathcal{A}P_k \\ a_k &= \|Q_{k-1}\|^2 / \|S_k\|^2 \\ X_k &= X_{k-1} + a_k P_k \end{aligned}$$

$$
\begin{aligned}
R_k &= R_{k-1} - a_k S_k \\
Q_k &= \mathcal{A}^* R_k \\
b_k &= \|Q_k\|^2 / \|Q_{k-1}\|^2 \\
P_{k+1} &= b_k P_k + Q_k
\end{aligned}
\tag{24}
$$

The convolution and correlation operations that are a part of $\mathcal{A}$ and $\mathcal{A}^*$ are evaluated by using the FFT. This, together with the fact that the storage requirements are reasonably modest, are the reasons why the conjugate gradient algorithm becomes attractive for large problems in our model.

We have used the above algorithm to solve a sample problem of 6144 unknowns of data type double complex (16 bytes each). With $\epsilon = 5 \times 10^{-2}$, convergence was achieved in 15 iterations, and a plot of *Test* is shown in Figure 3. The time for each iteration was 26 seconds. Of course, if ϵ is smaller, the solution may be "better," but the cost is increased iterations, making improved convergence rates of prime importance.

V. VALIDATION AND RESULTS

(a) Ferrite-Core Probe Model

Validation checks on the package have been done by self consistency testing, by comparing results with data computed directly from available analytical expressions, and by comparing field calculations with data obtained independently using a finite-element code designed for solving two-dimensional electromagnetic field problems [5,8]. Agreement with the two-dimensional finite-element code is important since it validates a crucial part of the package that determines the magnetization of ferromagnetic materials.

To give an example of an external validation, the electric field was determined for an axially symmetric ferrite-cored probe (core radius 0.25 mm, core length 10 mm, coil outer diameter 0.45 mm, coil inner diameter 0.25 mm and axial coil length 0.5 mm). The probe, shown in Figure 4, is based on a design for turbine disc inspection at 1 MHz on components of conductivity 0.82×10^6 S/m, and has a core of negligible conductivity, whose relative permeability is 200. The azimuthal electric field was computed using both a two-dimensional finite-element code [8] and our volume integral method. Figures 5 and 6 compare the real and imaginary parts of the field at the surface of the test piece for the two calculations, showing good agreement between the results.

Experimentally it has been shown that cup-cored probes, as in Figure 7, provide very good coupling with the workpiece, and are well suited for testing composite materials such as graphite-epoxy. Figure 8 shows the azimuthal electric field at the surface of an isotropic testpiece for zero lift-off, showing that the field is mainly confined within the probe region. An assessment of the coupling can be found from the normalized impedance characteristic, and it is important, therefore, that impedance calculations be included in the model. A normalized impedance diagram for the cup-core probe at various lift-off values is shown in Figure 9. These results were computed for the cup core probe above an isotropic half-space of conductivity 20,000 S/m.

(b) Flaw-Field Interaction

Validation of the code's ability to compute flaw-field interactions is continuing. In Figures 10 and 11 we compare the code's prediction of the impedance of a flaw (using (19)) with measured values, as a probe is scanned over the flaw. Clearly, the model is tracking the measurements well. Often this is all that is needed for problems of this type. This is a particular straightforward

application of the code, in that the matrix elements for the flaw need not be recomputed for each data point.

Even though the integral equations for the ferrite-core probe and flaw models are virtually identical, there are certain numerical details that differ. The principal one is that the computation of the matrix elements, via (14), is much more time consuming for the flaw than for the ferrite core. This is due to the fact that the dimensions of the flaw are much smaller than those of the core, which means that one must take many more data points in $k-$space in order to accurately evaluate (14) for the flaw than for the core. We are presently attempting to alleviate this problem by developing another scheme for computing the matrix elements for the flaw model.

VI. CONCLUSION

A comprehensive computer code for research and design studies in electromagnetic NDE is now at an advanced stage of development. It has the capability of predicting the impedance characteristics of three-dimensional flaws, and eddy-current probes in the presence of metals, semiconductors and advanced composites, as well as finding the electric and magnetic fields. By using a combination of the conjugate gradient method applied to a matrix, and FFT techniques, we have arrived at an algorithm that is both efficient in CPU time and has modest storage requirements. Pre- and post-processors are currently being developed to make the package available to the general user.

VII. ACKNOWLEDGEMENT

The authors are indebted to Dr. Steven Burke of Aeronautical Research Laboratories, Melbourne, Australia, for supplying the data shown in Figures 10 and 11.

This work was supported in part by The Naval Surface Weapons Center (White Oak Labs) under Contract No. N60921-86-C-0172 with Sabbagh Associates.

REFERENCES

1. Harold A. Sabbagh, "A Model of Eddy-Current Probes with Ferrite Cores," IEEE Trans. Magnetics, Vol. Mag-23, No. 3, May 1987, pp. 1888-1904.

2. J. R. Bowler, L. D. Sabbagh, and H. A. Sabbagh, "A Theoretical and Computational Model of Eddy-Current Probes Incorporating Volume Integral and Conjugate Gradient Methods," submitted to IEEE Trans. Magnetics.

3. J. R. Bowler, L. D. Sabbagh, and H. A. Sabbagh, "The Reduced Impedance Function for Cup-Core Eddy-Current Probes," submitted to IEEE Trans. Magnetics.

4. H. A. Sabbagh, L. D. Sabbagh and J. R. Bowler, "A Model of Ferrite-Core Probes Over Composite Workpieces," *Review of Progress in Quantitative Nondestructive Evaluation*, Vol.7A, D.O.Thompson and D.E.Chimenti, Eds. (Plenum, New York, 1988) pp. 479-486.

5. J. R. Bowler, "Eddy-Current Probe Interaction with Subsurface Cracks," *Review of Progress in Quantitative Nondestructive Evaluation,* Vol. 6A, D.O.Thompson and D.E.Chimenti, Eds. (Plenum, New York, 1987) pp. 185-191.

6. T. K. Sarkar, E. Arvas, and S. M. Rao, "Application of FFT and conjugate gradient method for the solution of electromagnetic radiation from electrically large and small bodies," IEEE Trans. Antennas and Propagation, Vol. AP-34, May 1986, pp. 635-640.

7. A. F. Peterson and R. Mittra, "On the Implementation and Performance of Iterative Methods for Computational Electromagnetics," Electromagnetic Communication Laboratory Technical Report No. 85-9, University of Illinois, Urbana, 1985.

8. A. G. A. Armstrong and C. S. Biddlecombe, "The PE2D package for transient eddy-current analysis," IEEE Trans. Magnetics, Vol. Mag-18, No.2, March 1982, pp. 411-415.

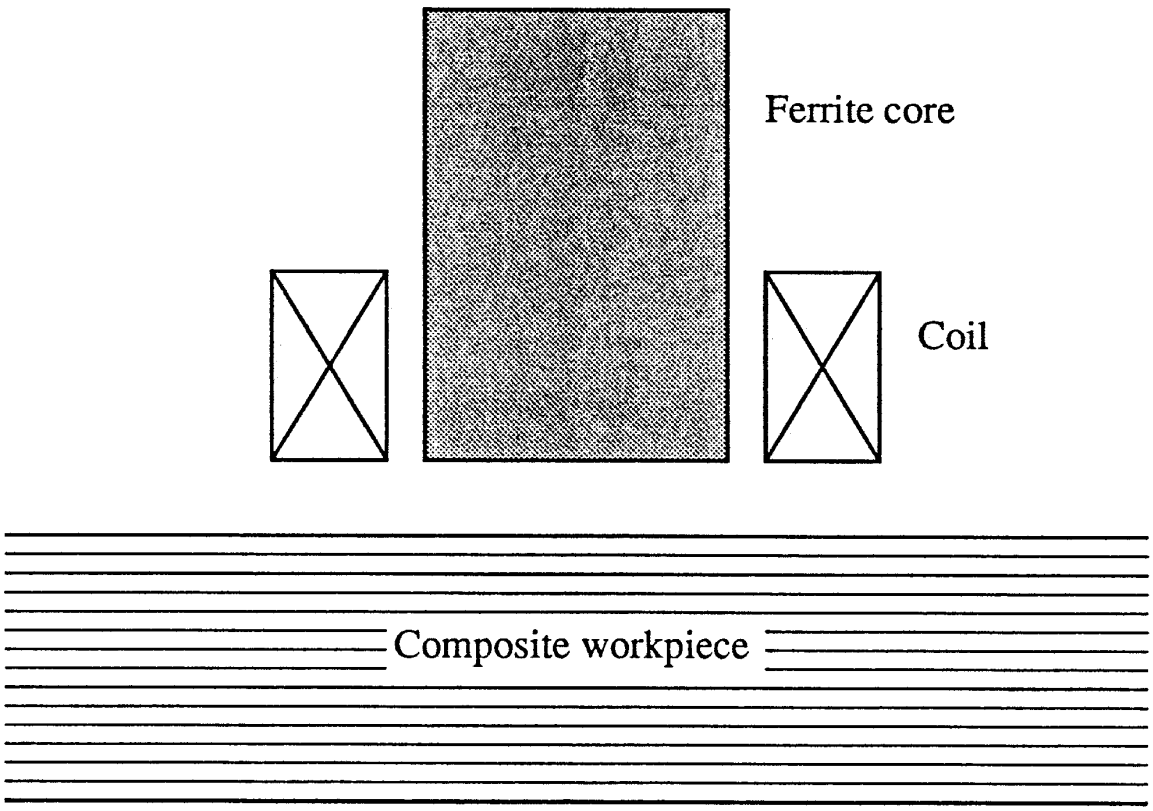

Figure 1. A ferrite core eddy-current probe over a stratified anisotropic workpiece.

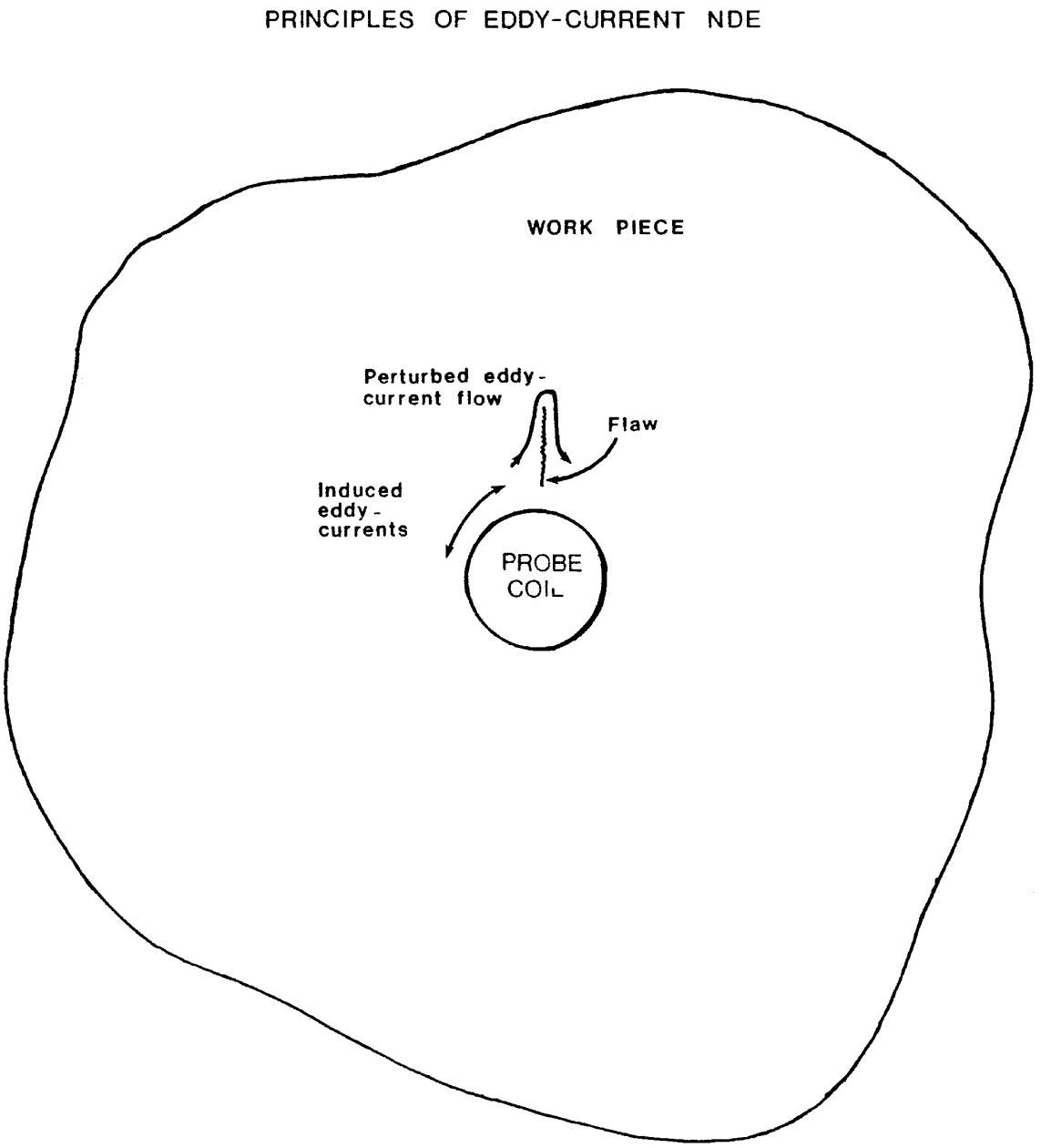

Figure 2. Showing a flaw as a perturbation of the workpiece (a conducting half-space).

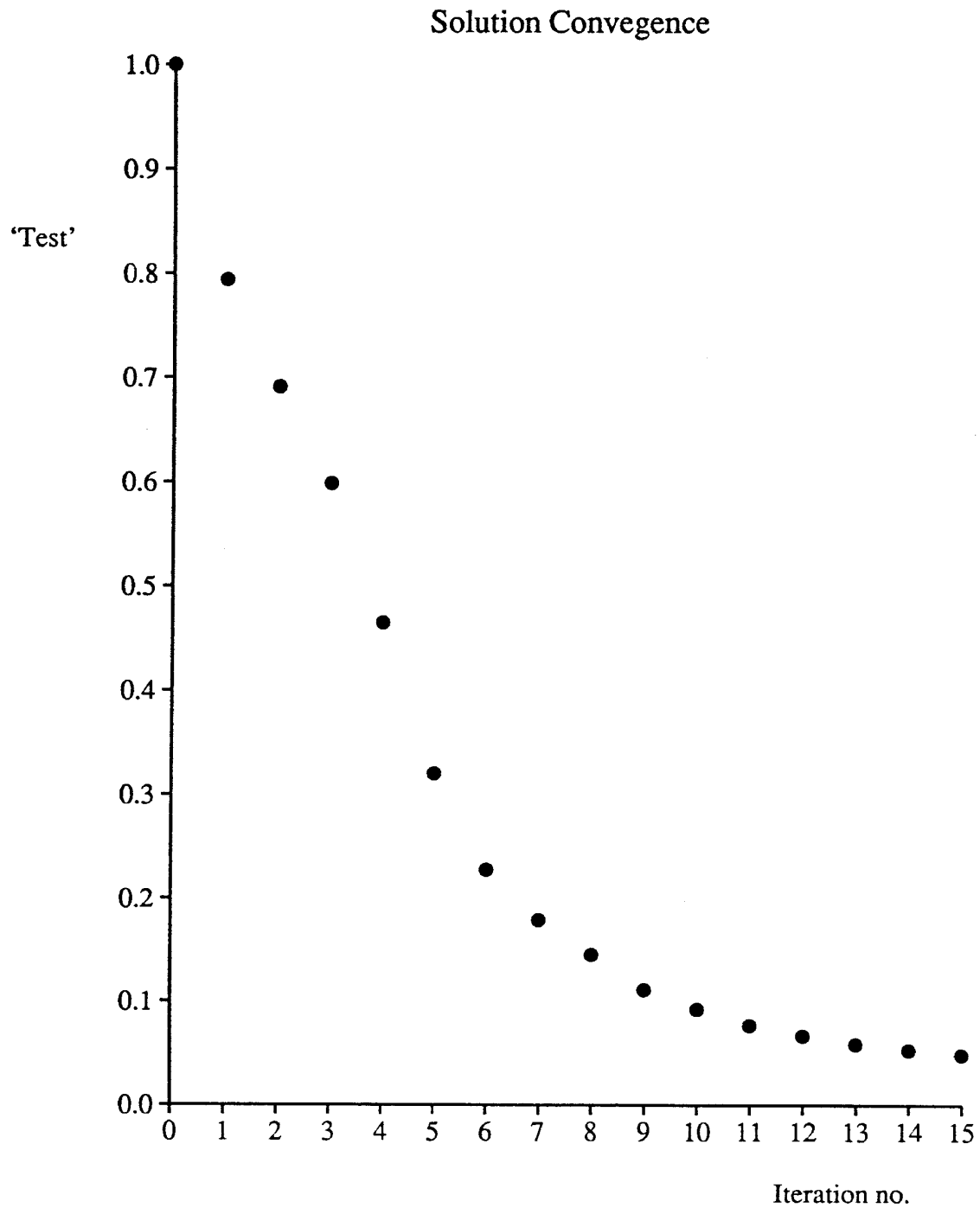

Figure 3. Convergence test for a problem of 6144 double-complex unknowns. The time for each iteration was 26 seconds.

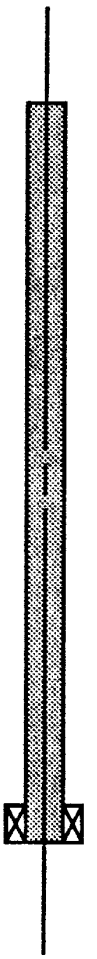

Figure 4. High resolution eddy-current probe. Core length $10mm$, diameter $0.5mm$, coil O/D $0.9mm$, I/D $0.5mm$, axial length of coil $0.5mm$.

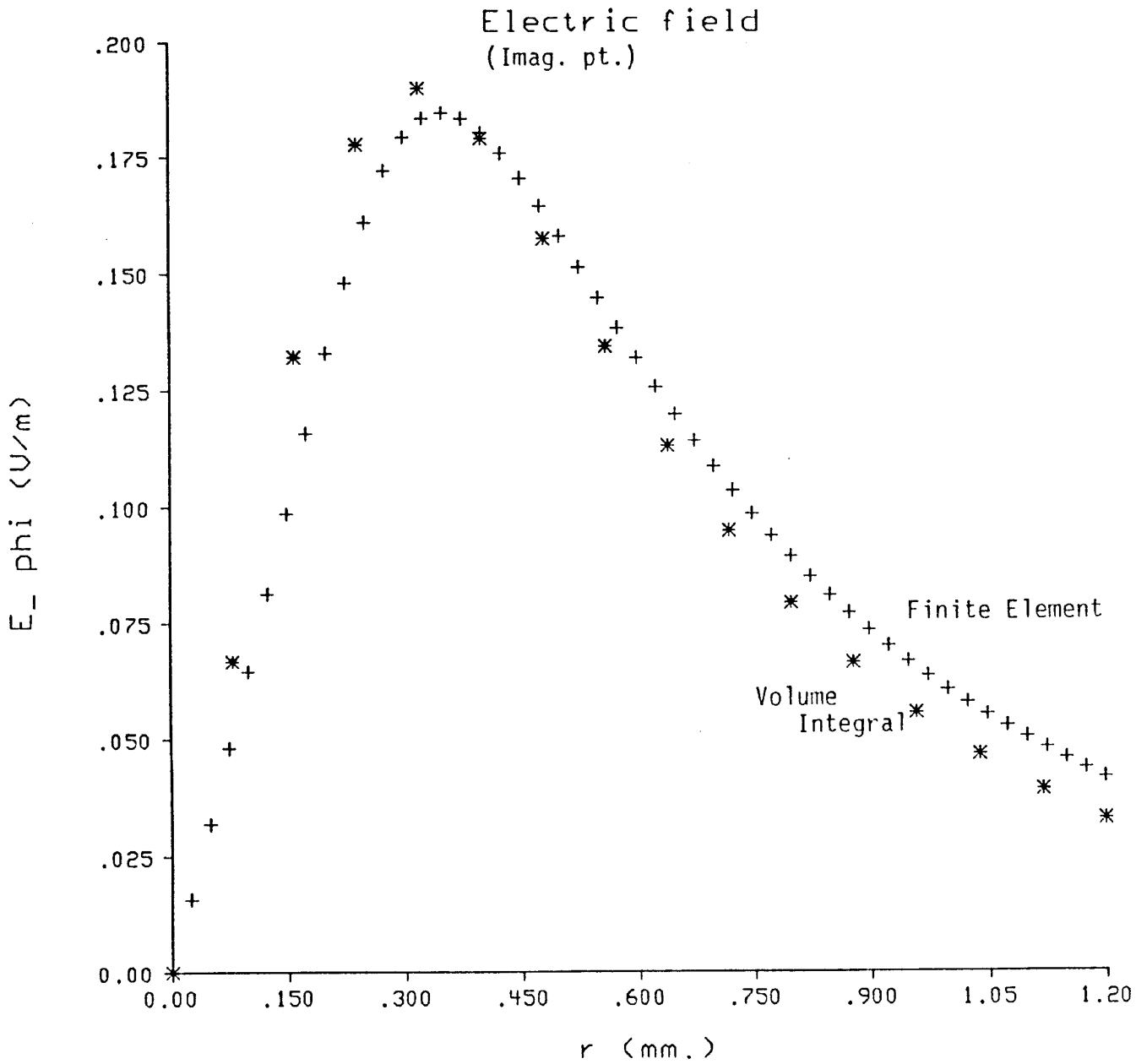

Figure 5. Radial variation of the azimuthal electric field, E_ϕ, at the surface of a homogeneous half-space conductor for the probe shown in Figure 4. Comparison of volume integral and finite element results: imaginary part.

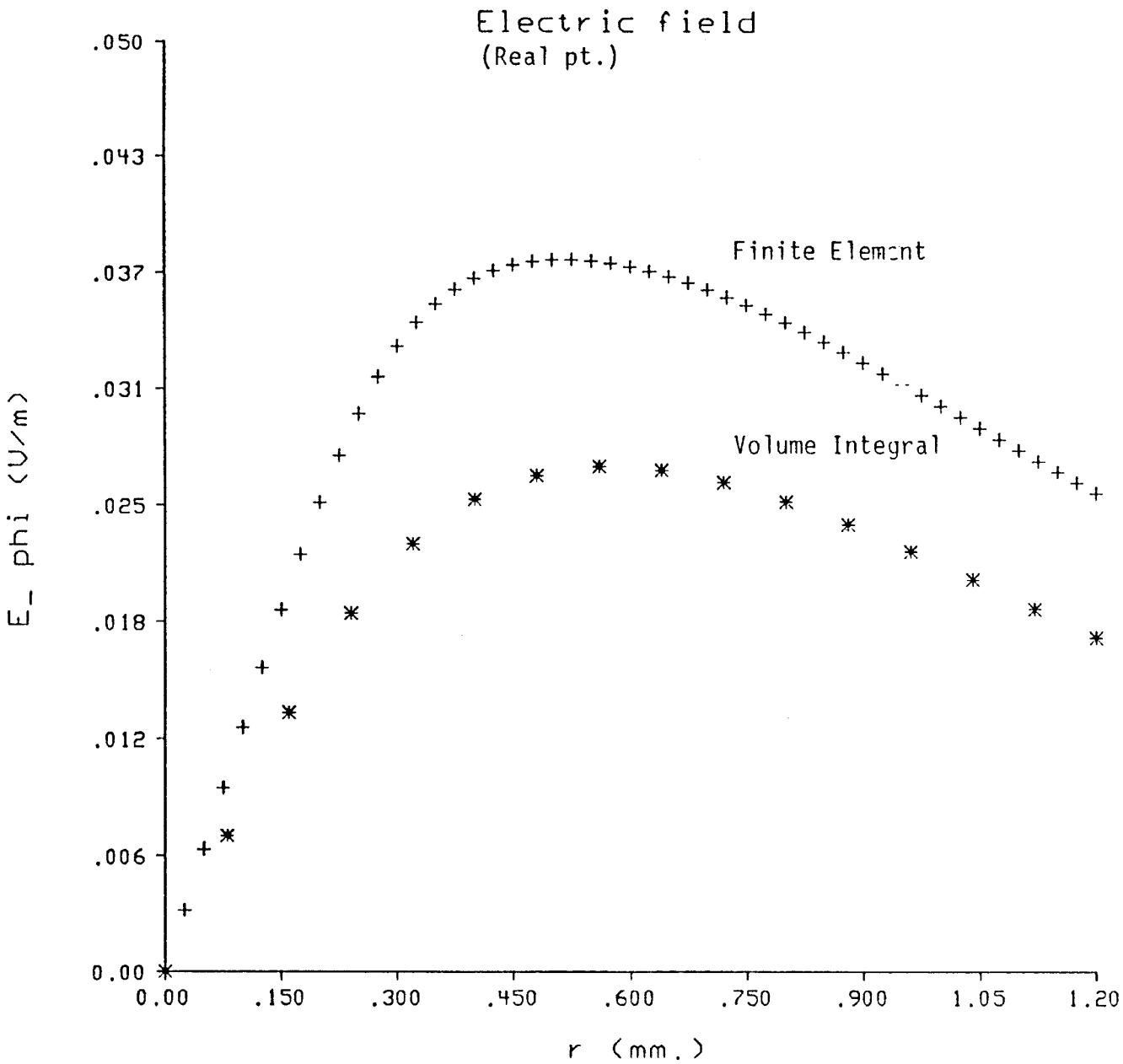

Figure 6. Radial variation of the azimuthal electric field, E_ϕ, at the surface of a homogeneous half-space conductor for the probe shown in Figure 4. Comparison of volume integral and finite element results: real part.

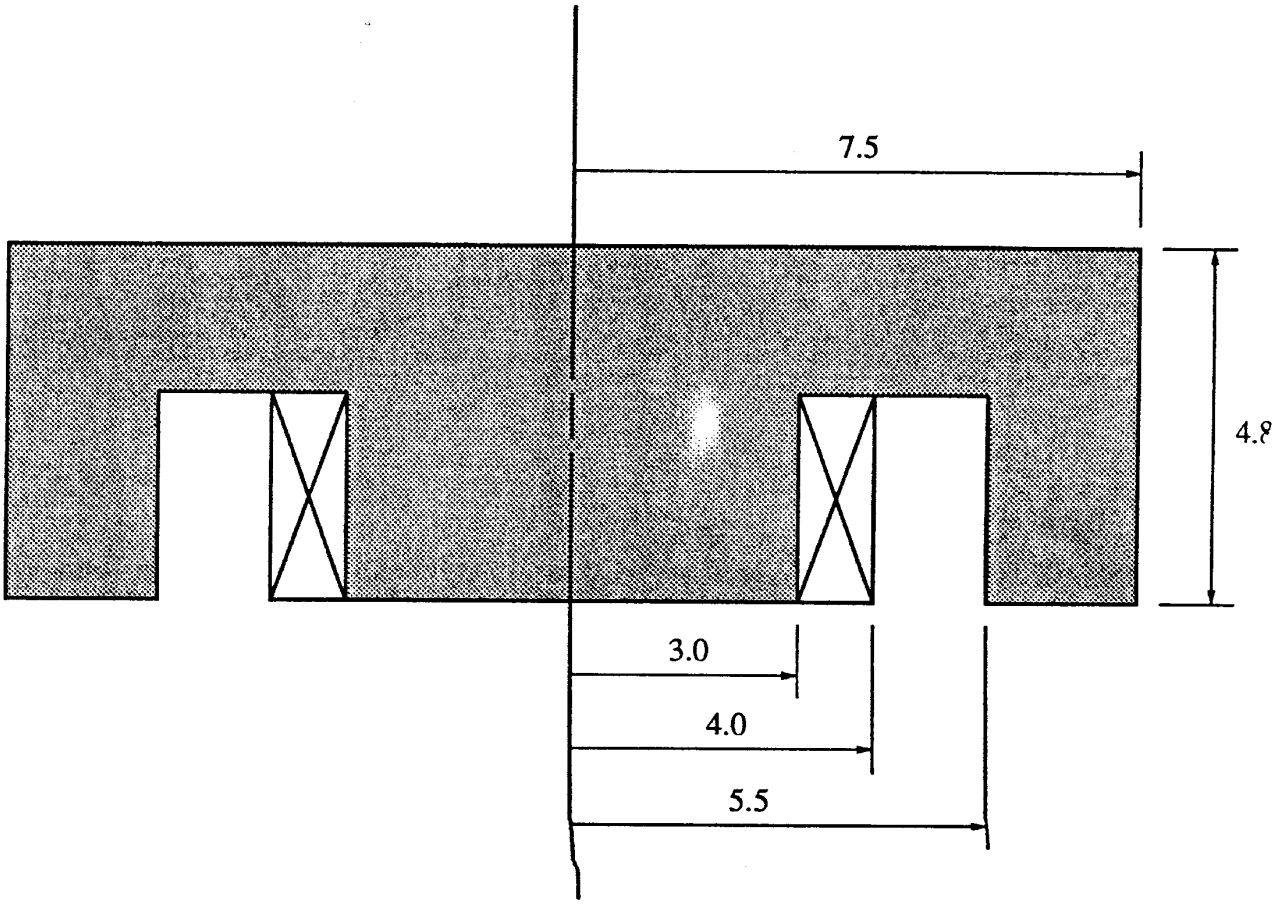

Figure 7. Cup core eddy-current probe of a type suitable for the inspection of graphite-epoxy. Dimensions are in mm. Typical operating frequency, $1MHz$.

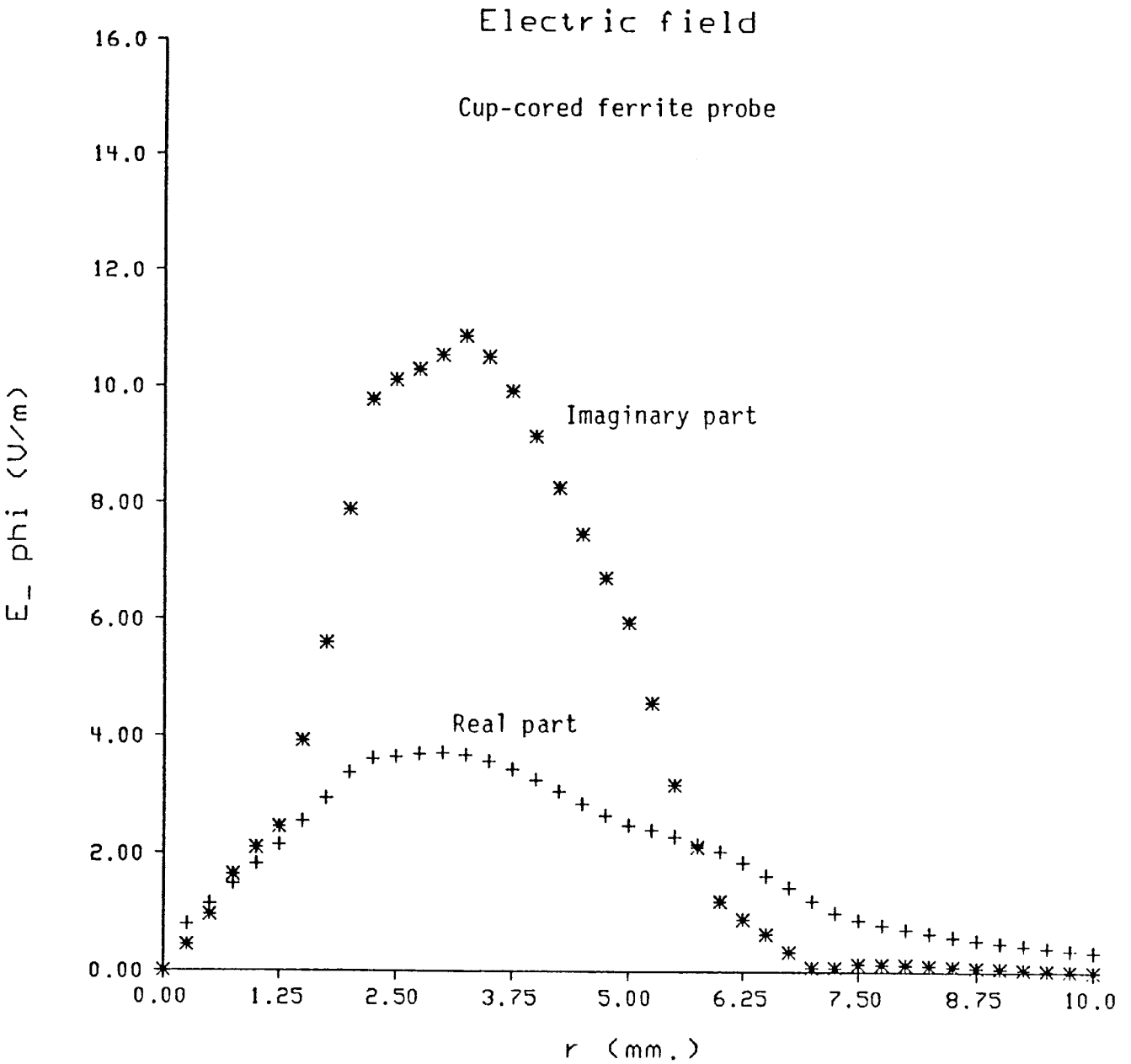

Figure 8. Radial variation of the azimuthal electric field, E_ϕ, at the surface of a homogeneous half-space conductor for the cup core probe shown in Figure 7.

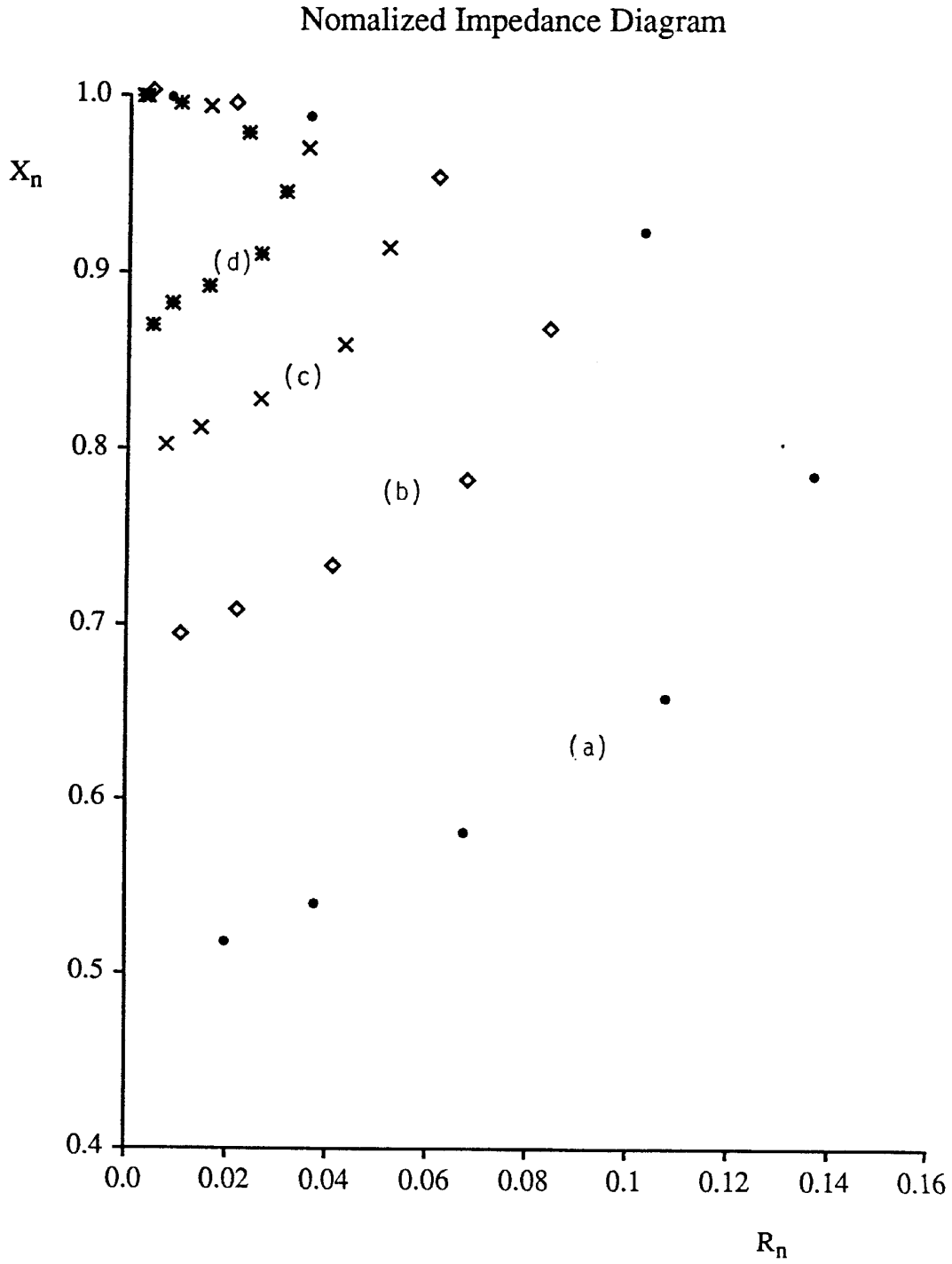

Figure 9. Normalised impedance characteristic for a cup core probe (Figure 7) above an isotropic workpiece of conductivity $20,000 Sm^{-1}$ for lift-off values (a) zero (b) $0.6mm$ (c) $1.2mm$ (d) $1.8mm$.

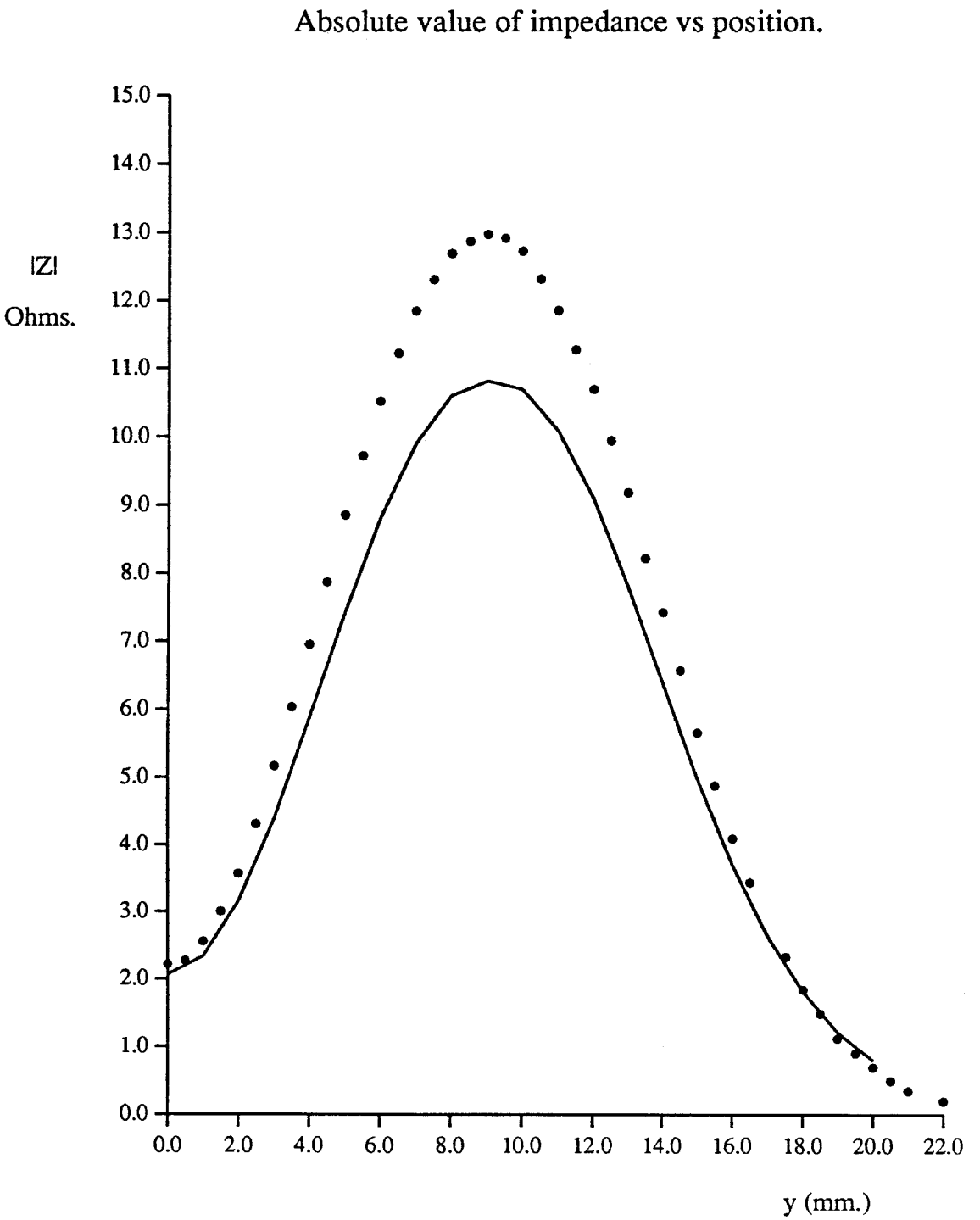

Figure 10. Comparison of the absolute value of flaw impedance vs. position of a probe coil. The solid curve is the model prediction, and the dots are measured values.

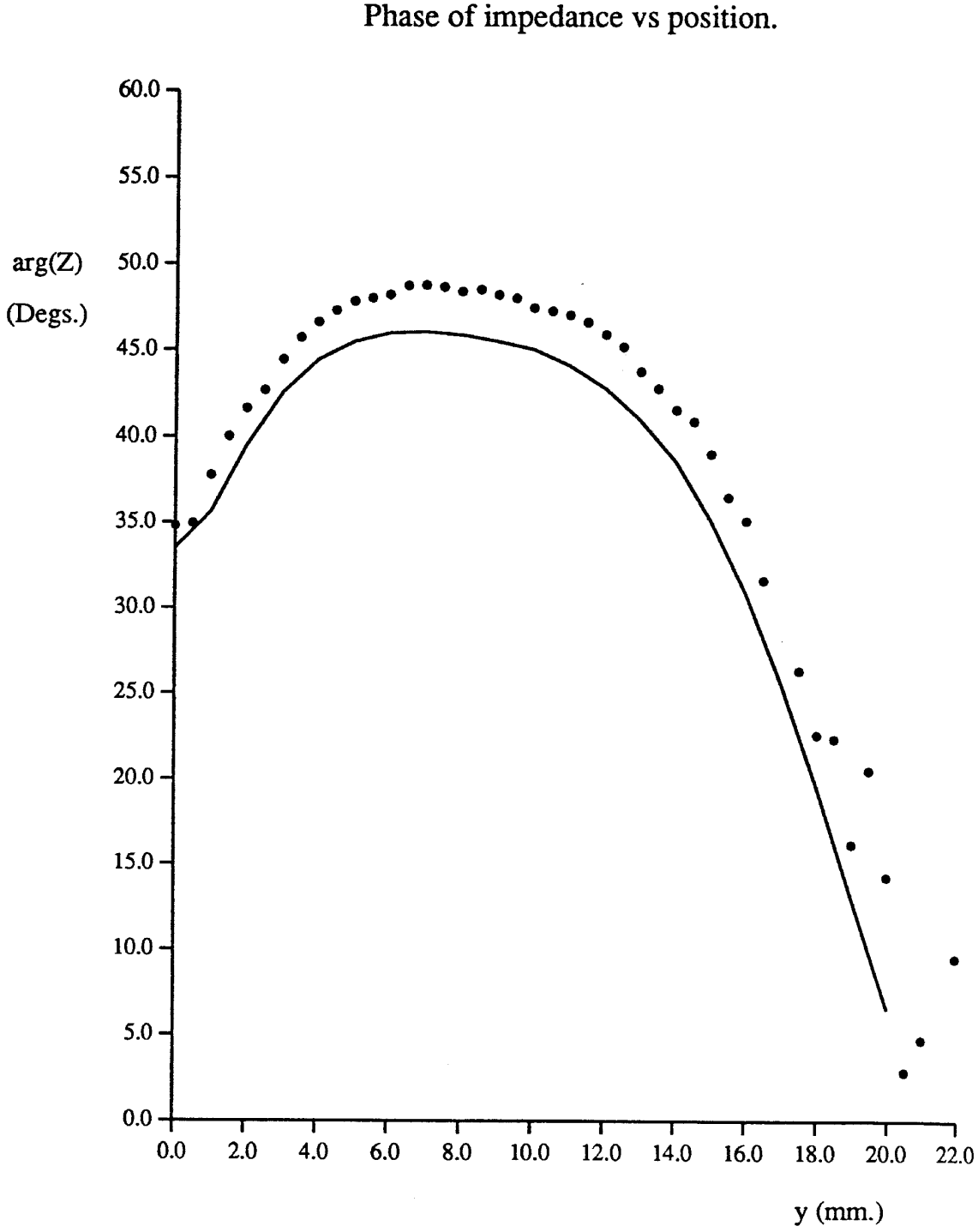

Figure 11. Comparison of the phase of flaw impedance vs. position of a probe coil. The solid curve is the model prediction, and the dots are measured values.